Hindawi Publishing Corporation
Discrete Dynamics in Nature and Society
Volume 2010, Article ID 569850, 16 pages
doi:10.1155/2010/569850

Research Article

Robust Controller Design Using the Nevanlinna-Pick Interpolation in Gyro Stabilized Pod

Bin Liu,[1,2] Chang-Hong Wang,[1] Wei Li,[1] and Zhuo Li[3]

[1] *Space Control and Inertial Technology Research Center, Harbin Institute of Technology, Harbin 150001, China*
[2] *School of Electric Information Engineering, Northeast Petroleum University, Daqing 163318, China*
[3] *College of Earth Science, Northeast Petroleum University, Daqing 163318, China*

Correspondence should be addressed to Bin Liu, liuzhen8936@yahoo.com.cn

Received 22 September 2010; Accepted 13 November 2010

Academic Editor: Li Xian Zhang

The sensitivity minimization of feedback system is solved based on the theory of Nevanlinna-Pick interpolation with degree constraint without using weighting functions. More details of the dynamic characteristic of second-order system investigated, which is determined by the location of spectral zeroes, the upper bound γ of S, the length of the spectral radius and the additional interpolation constraints. And the guidelines on how to tune the design parameters are provided. Gyro stabilized pod as a typical tracking system is studied, which is based on the typical structure of two-axis and four-frame. The robust controller is designed based on Nevanlinna-Pick interpolation with degree constraint. When both friction of LuGre model and disturbance exist, the closed-loop system has stronger disturbance rejection ability and high tracking precision. Numerical examples illustrate the potential of the method in designing robust controllers with relatively low degrees.

1. Introduction

Gyro stabilized pod can be used to isolate line of sight (LOS) from the movement and vibration of carrier and guarantee pointing and tracking for target in electro-optical tracking system, so in modern weapon systems it has been widely applied [1, 2]. The carrier vibration in the azimuth, pitch and roll direction induces the LOS of image sensor to rotate and causes the image blur and affects miss distance of the target, leading to the tracking performance degradation. In order to overcome these problems, we must establish a stable servosystem to isolate LOS from the movement and vibration of carrier, so as to guarantee system reliability and image quality [3]. The servosystem must not only have high precision and good dynamic quality, but also have disturbance rejection ability and large scale of adaptation range [4]. Along with improving control precision of gyro stabilized system, conventional methods have been limited, therefore, new design methods need to be found to improve system performance.

Up to now, PID control is still the most popular method applied in gyro stabilized pod. With the development of control technology in inertial system, a variety of control methods are produced, such as neural network control [5], Fuzzy control [6], H_∞ control [7], and optimal control [8], and they have gradually been applied to control the gyro stabilized platform. Switching control method has received much more attention recently, but still remaining at the theory analysis [9–11].

Weighting functions are adopted in conventional robust controller design, which are chosen to reflect the design objectives and the knowledge of the disturbances and sensor noise. In the optimal control design including H_2 and H_∞ control, a key step is the selection of weighting functions [12]. In many occasions, as in the scale case, the weights are chosen purely as a design parameter without any physical bases. What is worse is that the high order of weighting function will lead to high order of controller. Gahinet and Apkarian [13], and Skelton et al. [14] have introduced a technique for feedback design that allows such a constraint on the degree of the controller, in which performance and robustness are expressed by linear matrix inequalities. The relation between Nevanlinna-Pick (shortly denoted by NP) interpolation with degree constraint and sensitivity reduction is studied by Georgiou and Lindquist, which provides an alternative handle on McMillan degrees in feedback design [15]. The main difference between NP interpolation method and the existing H_∞ design methods is that the frequency weighting functions are not used to shape the frequency response of S. Another advantage of the method based on the NP interpolation theory is that controllers with relatively low degree can be obtained directly, without any model and controller reduction [16, 17].

Sensitivity minimization is one of the most fundamental and important issues in designing feedback system controllers. Although the idea of the application of NP theory with degree constraint to sensitivity, minimization was presented in [18]. Nagamune firstly gave the computation method for NP interpolation with degree constraint [19].

More details of the dynamic characteristic of second-order system is investigated in this paper, which is determined by the location of spectral zeroes, the upper bound γ of S, the length of the spectral radius, and the additional interpolation constraints. And the guidelines on how to tune the design parameters are provided.

This paper is organized as follows. In Section 2, the sensitivity reduction problem is revisited and it is reviewed how the problem is reduced to the NP interpolation problem. In Section 3, the NP interpolation theory with degree constraint is reviewed, and the dynamic characteristic of second-order system is investigated which is determined by the interpolation conditions. In Section 4, gyro stabilized pod as a typical tracking system is studied, which is based on the typical structure of two-axis and four-frame. The robust controller is designed based on NP interpolation with degree constraint.

2. Sensitivity Reduction of Tracking System and NP Interpolation

Considering a typical one degree of freedom stabilization system simplified to be suited to other applications such as stabilizing a sensor for electro-optical data gathering systems,

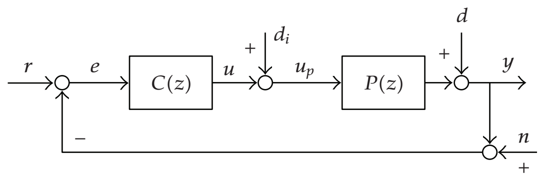

Figure 1: Configuration of feedback system.

the control configuration is shown in Figure 1. It consists of the interconnected $P(z)$ and the controller $C(z)$ forced by command r, sensor noise n, plant input disturbance d_i, and plant output disturbance d.

Without loss of generality, $P(z)$ is assumed to be real rational and proper, and all the unstable poles and zeroes of $P(z)$ are assumed to be simple and strictly outside the unit circle. Otherwise, [20–22] are referred for the reduction of cases with multiple and boundary zeroes and poles to this case.

Suppose that P has n_p poles and n_z zeroes in the closed right half plane (including point at infinity) let us denote them $p_1, p_2, \ldots, p_{n_p}$ and $z_1, z_2, \ldots, z_{n_z}$. If $n_p \neq 0$, P is unstable, which is needed to be stabilized by feedback. Therefore, a controller C is designed so that the closed-loop system fulfills certain design specifications, as depicted in Figure 1. It is well known that the transfer function from r to e that is called sensitivity function,

$$S = \frac{1}{1 + PC}, \tag{2.1}$$

which is also the transfer function from disturbance to the output, plays an important role in designing feedback controllers, that is because the frequency response of the sensitivity function determines the ability of the closed-loop system for disturbance rejection, tracking, robustness against noise and uncertainties, and so on.

The first object is to stabilize the tracking system in such a way that the transfer functions between any two arbitrary points in the closed-loop system is stable that is called internal stability. It is well known that internal stability can be guaranteed by the following Theorem 2.1.

Theorem 2.1 (see [23]). *Internal stability of tracking system is achieved if and only if the sensitivity function is stable and satisfies the interpolation conditions:*

$$\begin{aligned} &(1)\quad S(z_k) = 1, \quad k = 1, 2, \ldots, n_z, \\ &(2)\quad S(p_k) = 0, \quad k = 1, 2, \ldots, n_p. \end{aligned} \tag{2.2}$$

Secondly, a reduction of the H_∞-norm of S implies an attenuation of the effect of disturbances on the output since $\|y\|_2 \leq \|S\|_\infty \|d\|_2$. For robustness and tracking performance it is also desirable to put a specified uniform bound on the absolute value of the sensitivity function. For example, we need to bound $\|S\|_\infty \triangleq \sup_{\omega \in (-\infty, +\infty)} |S(j\omega)|$, since $\|e\|_2 \leq \|S\|_\infty \|r\|_2$. Therefore we require that $\|S\|_\infty < \gamma$ for some prescribed $\gamma > 0$.

With this bound, the suboptimal solution set to a scalar H_∞ control problem is equivalent to the solution set to the classical NP interpolation problem

$$S_{\mathrm{NP}} \triangleq \{S \in RH_\infty : \|S\|_\infty < \gamma,\ S(q_i) = w_i,\ i = 0, 1, \ldots, n\}. \tag{2.3}$$

By Pick's Theorem, this problem has a solution if and only if the Pick matrix

$$P \triangleq \left[\frac{1 - w_k \overline{w}_l}{1 - q_k^{-1} \overline{q}_l^{-1}}\right]_{k,l=0}^{n} > 0, \tag{2.4}$$

is positive definite [24].

3. NP Interpolation with Degree Constraint

3.1. Problem Formulation

For simplicity, we assume that the interpolation points, q_i, $i = 0, 1, \ldots, n$, are distinct and the interpolation values, w_i, $i = 1, \ldots, n$, are self-conjugate. Without loss of generality, we can also assume that $q_0 = \infty$ and that w_0 is real. The NP interpolation with degree constraint relating to the sensitivity function can be described as follows.

Given the sets of interpolation points and interpolation values $\{(q_i, w_i),\ i = 0, 1, \ldots, n\}$, $|q_i| > 1$, satisfying

$$P \triangleq \left[\frac{1 - w_k \overline{w}_l}{1 - q_k^{-1} \overline{q}_l^{-1}}\right]_{k,l=0}^{n} > 0, \tag{3.1}$$

a function from a subset of S_{NP}

$$S_{\mathrm{NPDC}} = S_{\mathrm{NP}} \cap S_{\mathrm{DC}}(n), \tag{3.2}$$

is desired, where $S_{\mathrm{DC}}(n) \triangleq \{S : \deg S \le n\}$.

The merit of bounding the degree of a closed-loop transfer function S is attributed to the following Theorem 3.1. And one of the main design parameters of S is stated in Theorem 3.2, which are called the spectral zeros.

Theorem 3.1 (see [25]). *Suppose P is strictly proper and that S satisfies the interpolation conditions* (2.2). *Then the controller*

$$C = \frac{1 - S}{PS} \tag{3.3}$$

satisfies the degree bound

$$\deg C \le \deg P - n_z - n_p + \deg S, \tag{3.4}$$

where n_z and n_p are the number of unstable zeros and poles of P, respectively.

Theorem 3.2 (see [16]). *For each monic real stable polynomial:*

$$\rho(z) = z^n + \rho_1 z^{n-1} + \cdots + \rho_n, \tag{3.5}$$

there exists a unique pair of real polynomials:

$$\begin{aligned} a(z) &= a_0 z^n + a_1 z^{n-1} + \cdots + a_n, \quad a_0 > 0, \\ b(z) &= b_0 z^n + b_1 z^{n-1} + \cdots + b_n, \quad b_0 > 0 \end{aligned} \tag{3.6}$$

which satisfy

(1) $S(z) = b(z)/a(z)$ *is strictly bounded real,*

(2) $S(q_i) = w_i$, $i = 0, 1, \ldots, n$,

(3) $\gamma - S(z)S(z^{-1}) = \rho(z)\rho(z^{-1})/a(z)a(z^{-1})$.

In other words, for each $\rho(z)$, there exists a unique solution $S(z)$ to the NP problem with degree constraint. In addition, the relation between the set of self-conjugate n zeros of $\rho(z)$ inside the unit circle in the complex plane and the set of the solution pairs $(a(z), b(z))$ of the NP problem with degree constraint is bijective. In particular, zeros of $\rho(z)$ is called the spectral zeros of the function $S(z)$, and the distance between the spectral zero and the origin is called the spectral radius. In [16], it is shown how to determine the unique $S(z)$ numerically from the set of spectral zeros of the function $S(z)$ by transforming the infinite dimensional entropy maximization problem into a dual finite dimensional strictly convex minimization problem.

If it is impossible to find an $S(z)$ meeting $\|S\|_\infty < \gamma$ by using the spectral zeros, we must introduce extra interpolation constraints:

$$S(\lambda_i) = \alpha_i, \quad i = 1, \ldots, n_e, \tag{3.7}$$

where $|\lambda_i| > 1$. That is the degree bound of $S(z)$ will be raised. Then the NP interpolation with degree constraint is redefined as

$$S_{\text{NPDC}} = S_{\text{NP}} \cap \{S : S(\lambda_i) = \alpha_i, i = 1, 2, \ldots, n_e\} \cap S_{\text{DC}}(n + n_e). \tag{3.8}$$

The additional interpolation sets can be chosen freely except with conditions that they do not violating the positivity of the corresponding Pick matrix and that the total interpolation data set forms self-conjugate pairs, if they are not real. It is also important to note that additional interpolation constraints can influence both gain and phase of $S(z)$. Next, the relation between the location of the spectral zeros/additional constrains and the shape of the corresponding $|S(z)|$.

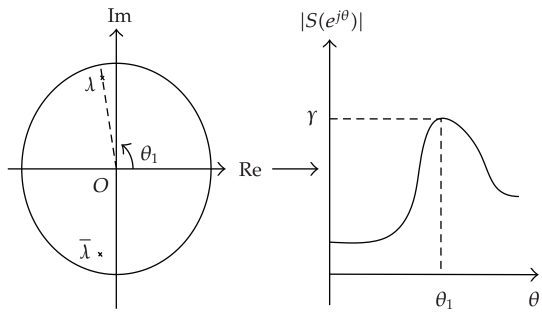

Figure 2: Influences of a spectral zero λ on $|S(z)|$.

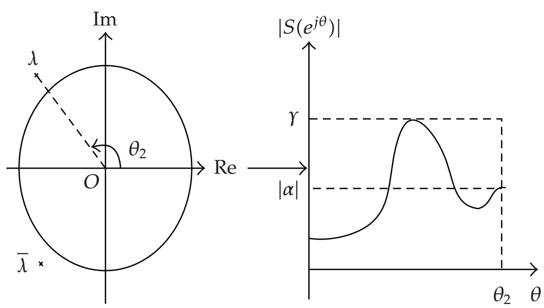

Figure 3: Influences of an extra interpolation constraint $S(\lambda) = \alpha$ on $|S(z)|$.

3.2. The Relation between Spectral Zeros and $|S(z)|$

If the spectral zero λ locates near the unit circle $z = e^{j\theta_1}$, it will lifts $|S(z)|$ up to the level near the upper bound γ at the frequency θ_1, as depicted in Figure 2. This is because if λ is a spectral zero close to the unit circle $z = e^{j\theta_1}$,

$$\Gamma(\lambda) = \gamma^2 - S(\lambda)S\left(\lambda^{-1}\right) = 0, \tag{3.9}$$

and hence $|S(e^{j\theta_1})| \approx \gamma$. Then, by the water-bed effect, the sensitivity will often be lowered in other parts of the spectrum [9].

3.3. The Relation between Extra Interpolation Constraints and $|S(z)|$

Introducing an extra interpolation condition $S(\lambda) = \alpha$, where λ is close to $z = e^{j\theta_2}$, fixes the modulus of the sensitivity at a level close to $|\alpha|$ and the phase of $|S(z)|$ close to that of α at the frequency θ_1, as depicted in Figure 3. Thus, (λ, α) can control the magnitude $|S(z)|$ and the phase of the sensitivity. However, the more extra interpolation constraints, the larger bound of $\deg(S)$. From Theorem 3.1, the controller degree bound will increase by the number of extra interpolation constraints. Thus, we should try to use additional constraints as little as possible.

3.4. The Relation between NP Interpolation Conditions and the Dynamic Characteristic

In this section, we will propose general strategies to tune the design parameters by investigating the relation between NP interpolation conditions and the dynamic characteristic of second-order system.

Suppose the continuous-time plant described by

$$P(s) = \frac{1-s}{s^2+s+1}, \tag{3.10}$$

and the H_∞ norm bound constraint

$$\|S\|_\infty < 2. \tag{3.11}$$

First, by Möbius transform: $s = (z-1)/(z+1)$, which conformally maps the right half plane into the complement of the unit disk:

$$P(z) = \frac{2(z+1)}{3z^2+1}, \tag{3.12}$$

the set of corresponding to S_{NPDC} is obtained in the discrete-time setting

$$S_{\mathrm{NPDC}} \triangleq \{S \in RH_\infty, \|S\|_\infty < 2, S(-1) = 1, S(\infty) = 1\} \cap S_{\mathrm{DC}}(1). \tag{3.13}$$

Note that the condition $S(-1) = 1$ in (3.13) is a boundary interpolation constraint, which makes the NP interpolation problem complicated. This difficulty can be circumvented by introducing another variable $\varepsilon > 0$. Define a new function as follows:

$$\tilde{S}(z) \triangleq S\left(\frac{z}{1+\varepsilon}\right), \tag{3.14}$$

the NP interpolation with degree constraint becomes

$$\tilde{S}_{\mathrm{NPDC}} \triangleq \left\{\tilde{S} \in RH_\infty, \left\|\tilde{S}\right\|_\infty < 2, \tilde{S}(-1 \times (1+\varepsilon)) = 1, \tilde{S}(\infty) = 1\right\} \cap S_{\mathrm{DC}}(1). \tag{3.15}$$

If $\varepsilon = 0.005$, the set (3.15) will be

$$\tilde{S}_{\mathrm{NPDC}} \triangleq \left\{\tilde{S} \in RH_\infty, \left\|\tilde{S}\right\|_\infty < 2, \tilde{S}(-1.005) = 1, \tilde{S}(\infty) = 1\right\} \cap S_{\mathrm{DC}}(1). \tag{3.16}$$

Especially, we will introduce an extra interpolation condition to investigate the influence to dynamic characteristic of second-order system. We choose $\tilde{S}(1.002) = 0$ as the adding constraint. The NP interpolation problem with degree constraint is redefined as

$$\tilde{S}_{\mathrm{NPDC}} \triangleq \left\{\tilde{S} \in RH_\infty, \left\|\tilde{S}\right\|_\infty < 2, \tilde{S}(-1.005) = 1, \tilde{S}(\infty) = 1, \tilde{S}(1.002) = 0\right\} \cap S_{\mathrm{DC}}(2). \tag{3.17}$$

Next, we will study how the following four factors influence the dynamic characteristic of second-order system: the location of the spectral zeros, the upper bound γ of $\|S\|_\infty$, the length of spectral radius, and the additional constrains.

(a) The Influence of the Location of the Spectral Zeros.

When we locate 5 groups spectral zeros: $0.97e^{\pm 0.1i}$, $0.97e^{\pm 0.785i}$, $0.97e^{\pm 1.57i}$, $0.97e^{\pm 2.355i}$, $0.97e^{\pm 3i}$, which are self-conjugate, and of the same length of spectral radius, the corresponding step response of closed-loop system is depicted in Figure 4, denoted by y_1, y_2, y_3, y_4, y_5. The closer to positive real semiaxis the spectral zeros, the larger the overshoot and the longer the settling time t_s. When the spectral zeros are located in left half plane, there is no overshoot, and the settling time becomes shorter. For the described plant (3.10), when the located spectral zeros are near the positive real semiaxis, the settling time is about 180 seconds. When they are near the negative real semiaxis, the settling time is about 5 seconds, but the undershoot becomes larger. In the following (b), (c), (d), the spectral zeros are chosen as $\pm 0.97i$.

(b) The Influence of the upper bound γ of $\|S\|_\infty$.

The upper bound γ of $\|S\|_\infty$ is specified as 1.1, 2, 5, 8, 9. The corresponding step responses are depicted in Figure 5, denoted by y_1, y_2, y_3, y_4, y_5. When γ is close to 1, the closed-loop system becomes unstable. Increasing the value of γ, the overshoot becomes larger. The rise times t_r are almost the same. For the given plant (3.10), $\gamma = 2$ is appropriate.

(c) The Influence of the length of spectral radius.

When we choose the spectral zeros: $\pm 0.2i$, $\pm 0.5i$, $\pm 0.97i$, they have the same phase lying in imaginary axis. However, they have different distance from to origin. Three step response curve are depicted in Figure 6, denoted by y_1, y_2, y_3. As we can see, the rise time t_r becomes longer with the spectral radius smaller. When the spectral radius is less than 0.5, there is no overshoot.

(d) The Influence of the additional constrains.

The extra interpolation conditions are chosen as 1.5, 1.2, 1.1, 1.05, 1.01, 1.005, 1.002, 1.0005. Their step responses are depicted in Figure 7, denoted by y_i, $i = 1, \ldots, 8$. The settling time t_s is almost unchanged. But, the steady error becomes larger with the value of the additional interpolation points increasing.

The location of spectral zeros and the upper bound γ of $\|S\|_\infty$ have more influence to the overshoot and the settling time of feedback system. The spectral zeros should be located in the left half plane, and the less γ, the better, if the closed-loop system is stable. The spectral radius affects the dynamic characteristic little except only some influence to the rise time. The additional interpolation conditions have more impact on the steady error, and the extra interpolation points of less value should be chosen from the simulation. We will mainly utilize these four strategies for controller design, instead of using weighting functions.

4. Example Illustrating the New Design Method

4.1. Mathematical Model of Gyro Stabilized Pod

The gyro stabilized pod investigated in this paper is based on the typical structure of two-axis and four-frame. The stabilization loop of each axis is almost the same, including stabilization controller, motor drive circuits, DC torque motor, and rate gyro. Take the pitch framework for example, the block diagram of stabilization loop is as in Figure 8, where

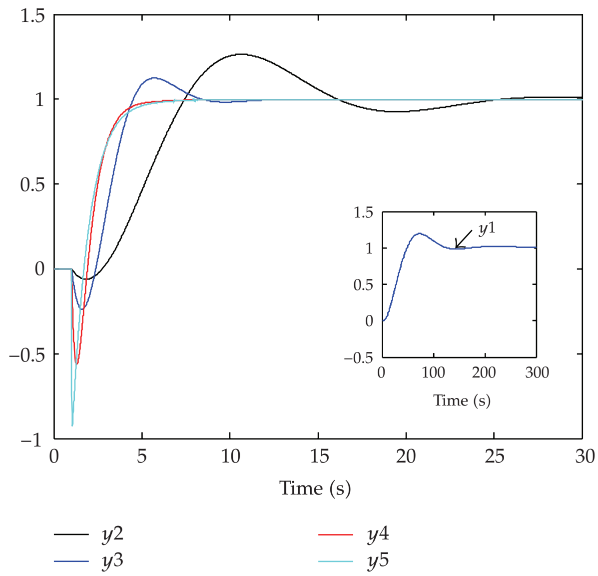

Figure 4: The influence of the location of the spectral zeros.

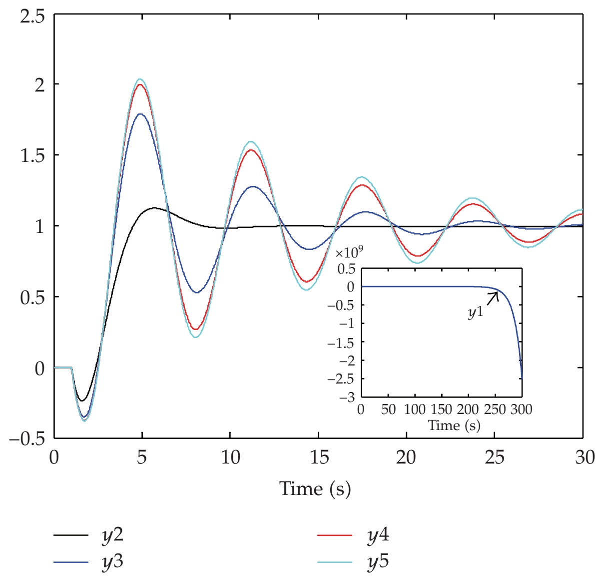

Figure 5: The influence of the upper bound γ of $\|S\|_\infty$.

$G_c(s)$ is the transfer function of correction link. v represents friction torque disturbance. w represents measurement noise. The approximate open-loop transfer function of the plant:

$$P(s) = \frac{3s + 1.6}{10s^2 + 17s + 6}. \tag{4.1}$$

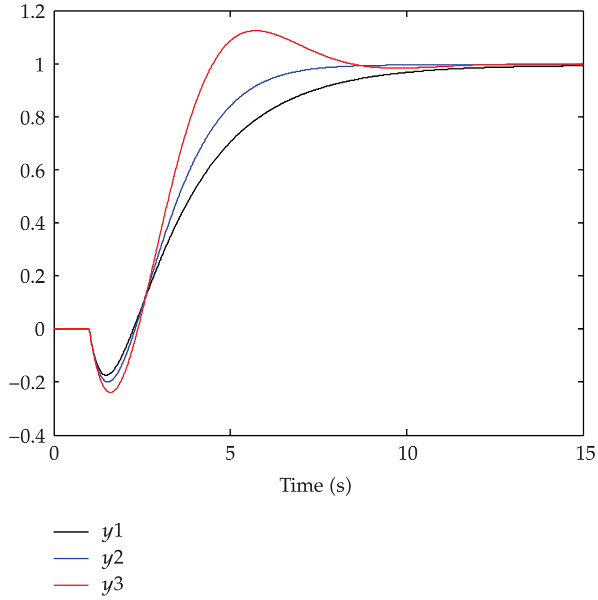

Figure 6: The influence of the length of spectral radius.

Design requirements:

(R1) overshoot: $\sigma\% \leq 10\%$;

(R2) settling time: $t_s \leq 0.1$ sec;

(R3) oscillatory times: $N < 2$;

(R4) steady-state error of system approaches zero.

In this subsection, the robust control problem is solved by the proposed method. The plant treated is transformed from (4.1)

$$P(z) = \frac{23(z+1)(z-0.3043)}{165(z-0.3043)(z+0.0909)}, \tag{4.2}$$

which has a bound unstable zero $S(-1) = 1$. The upper bound of the $\|S\|_\infty$ can be chosen 1.7. The set of functions meeting the interpolation constraints is represented as

$$S_{\mathrm{NPDC}} \triangleq \{S \in RH_\infty, \|S\|_\infty < 1.7, S(-1) = 1\} \cap S_{\mathrm{DC}}(0). \tag{4.3}$$

As described in Section 3.4, we introduce the variable $\varepsilon = 0.005 > 0$, and defined another set of functions:

$$\widetilde{S}_{\mathrm{NPDC}} \triangleq \left\{\widetilde{S} \in RH_\infty, \left\|\widetilde{S}\right\|_\infty < 1.7, \widetilde{S}(-1.005) = 1\right\} \cap S_{\mathrm{DC}}(0). \tag{4.4}$$

It can be shown that the set $\widetilde{S}_{\mathrm{NPDC}}$ has only one element, namely, $\widetilde{S}_{\mathrm{NPDC}} \triangleq \{\widetilde{S} : \widetilde{S} \equiv 1\}$, which does not satisfy design requirements. Hence, it is necessary to add some

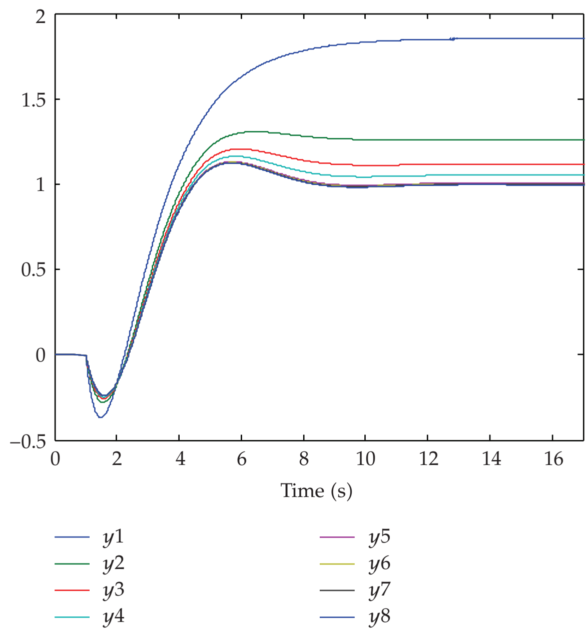

Figure 7: The influence of the additional constrains.

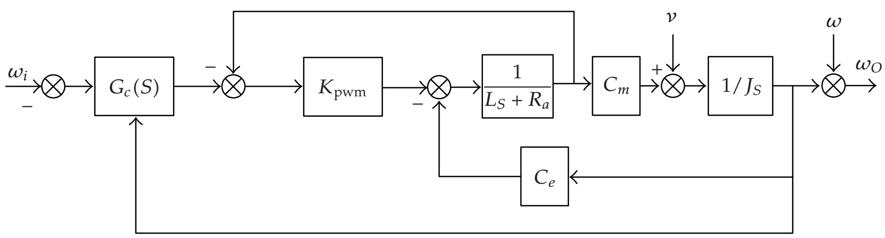

Figure 8: Block diagram of stabilization loop.

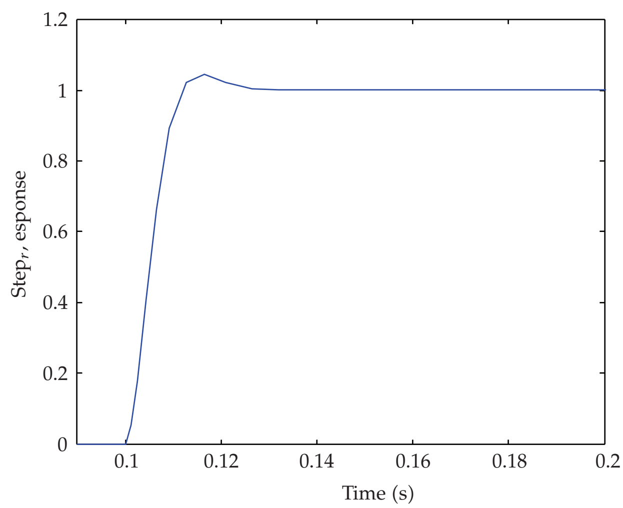

Figure 9: Step response of tracking system.

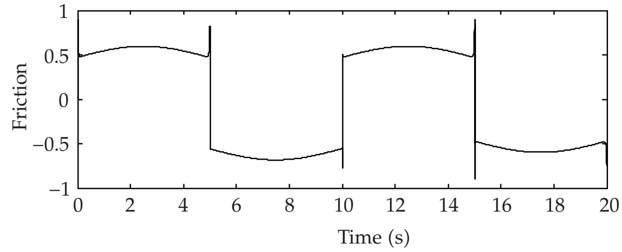

(a)

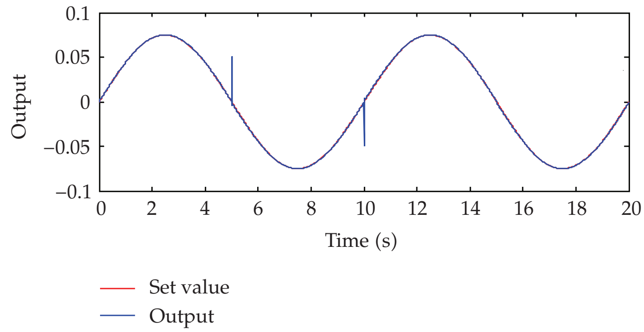

(b)

Figure 10: Reference signal is sinusoidal signal of 0.1 Hz.

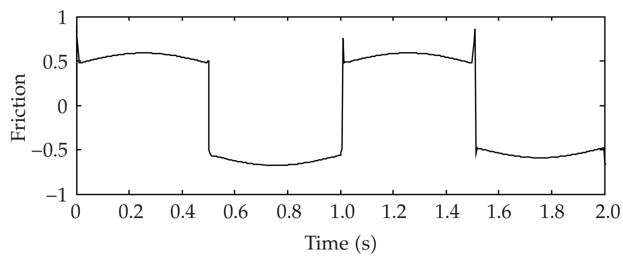

(a)

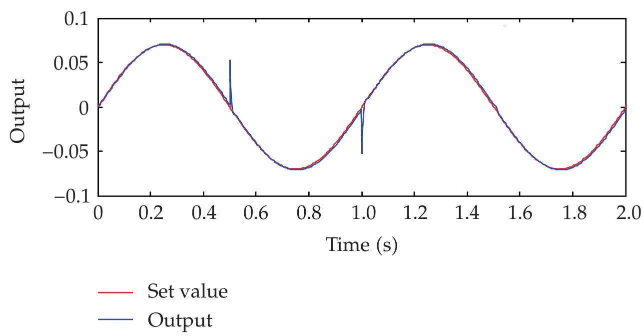

(b)

Figure 11: Reference signal is sinusoidal signal of 1 Hz.

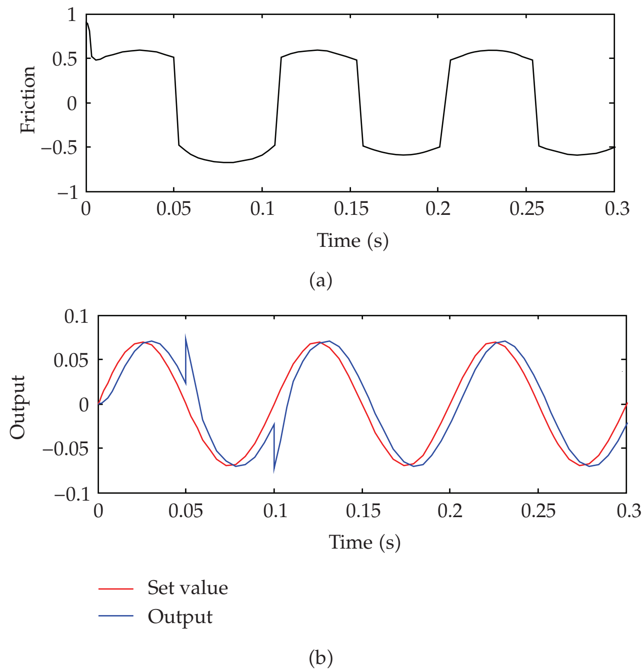

Figure 12: Reference signal is sinusoidal signal of 10 Hz.

interpolation constraints for the achievement of the specification. Taking into account the low gain requirement at low frequencies, we introduce one additional interpolation constraint $\widetilde{S}(1.005) = 0$, and redefine the set $\widetilde{S}_{\text{NPDC}}$ by

$$\widetilde{S}_{\text{NPDC}} \triangleq \left\{ \widetilde{S} \in RH_{\infty}, \left\| \widetilde{S} \right\|_{\infty} < 1.7, \widetilde{S}(-1.005) = 1, \widetilde{S}(1.005) = 0 \right\} \cap S_{\text{DC}}(1). \tag{4.5}$$

Now we have one spectral zero of the function $1.7^2 - \widetilde{S}(z)\widetilde{S}(z^{-1})$ as the design parameter. When the spectral zero is located at $z = -0.98$, the corresponding sensitivity function is calculated as

$$\widetilde{S}(z) = \frac{0.00602z - 0.00605}{z + 0.9929}. \tag{4.6}$$

Due to the reverse variable transform, the sensitivity function corresponding to (4.6) becomes

$$S(s) = \widetilde{S}\left((1+\varepsilon)\frac{1+s}{1-s} \right) = \frac{s}{s + 165.1143}. \tag{4.7}$$

And, the controller calculated by (3.3) is

$$C(s) = \frac{1651.143(s^2 + 1.7s + 0.6)}{3s^2 + 1.6s}. \tag{4.8}$$

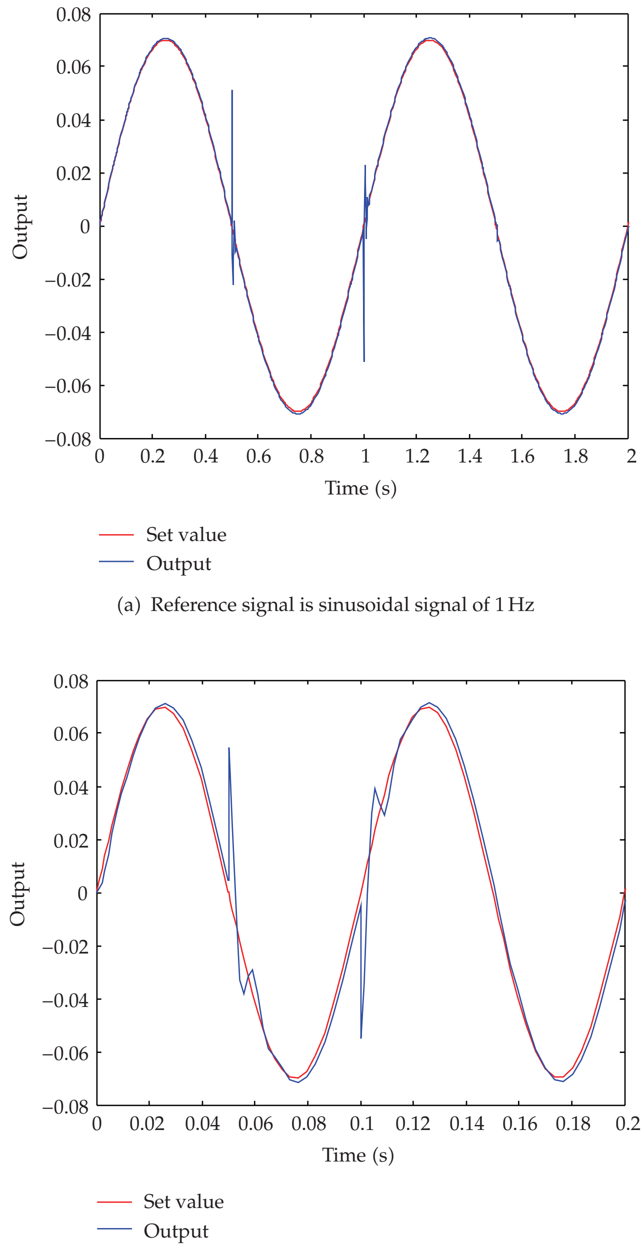

(a) Reference signal is sinusoidal signal of 1 Hz

(b) Reference signal is sinusoidal signal of 10 Hz

Figure 13: Output curves of different frequency.

4.2. Tracking Performance and Disturbances Rejection

As can be seen in Figure 9, design requirements (R1)–(R4) are all met. Next, we will check the tracking performance and the disturbance rejection ability using sinusoidal signal of three different frequencies: 0.1 Hz, 1 Hz, 10 Hz. Both the friction and the pulse jamming are considered simultaneously. The friction torque is described by LuGre model

$$T_f = \left(T_c + (T_s - T_c)e^{-(\dot{\theta}/\dot{\theta}_s)^2}\right)\operatorname{sgn}(\dot{\theta}) + \sigma_2\dot{\theta}, \tag{4.9}$$

where T_s is static friction force, T_c is Coulomb friction force, $\dot{\theta}_s$ is Stribeck velocity, σ_2 is viscous friction coefficient, and $\dot{\theta}$ is angular velocity. Obviously, the friction force will be different when tracking different frequency sinusoidal signal, as depicted in Figures 10–12. The pulse jamming is inserted into the output of the plant at $t = 5$ sec, 0.5 sec, 0.05 sec, and the lasting time is 5 sec, 0.5 sec, and 0.05 sec.

As can be seen in Figures 10–12, the proposed method has advantages of short regulating time, high precision, and high disturbance rejection ability.

4.3. Influence of Model Uncertainty to Tracking Performance

Suppose that the perturbed plant is described by

$$\widetilde{P}(s) = \frac{5s^2 + 3s + 1.6}{3s^3 + 10s^2 + 17s + 6}. \tag{4.10}$$

Sinusoidal signals of different frequency, 1 Hz, 10 Hz, are adopted as the reference signal. The disturbances are the same as in Section 4.2. The main difference between Figures 11(b), 12(b) and 13 is that the later has longer settling time when the pulse jamming is added to the output of the plant. The Oscillatory times become more and more when the plant has uncertainty.

5. Conclusions

In this paper, we have proposed a new approach to the robust controller design based on the NP interpolation theory with degree constraint. There are two kinds of design parameters: the spectral zeros and the extra interpolation constrains. We have investigated how the following four factors influence the dynamic characteristic of second-order system: the location of the spectral zeros, the upper bound γ of $\|S\|_\infty$, the length of spectral radius, and the additional constrains. And we also provide the guidelines on how to tune the design parameters. Gyro stabilized pod as a typical tracking system is studied. Simulations show that the proposed method has advantages of short regulating time, high precision, strong disturbance rejection ability, and good robustness.

References

[1] W. Ji and Q. Li, “Adaptive fuzzy PID control for LOS stabilization system on gyro stabilized platform,” *Acta Aeronautica et Astronautica Sinica*, vol. 28, no. 1, pp. 191–195, 2007.
[2] M. K. Loh, *Design, Development and Control of a LOS Stabilization System*, National University of Singapore, Singapore, 1991.
[3] J. Kun, *Design and Research on Stabilization Loop of Gyro Stabilized POD Control System*, Harbin Institute of Technology, Harbin, China, 2008.

[4] K. Murphy, S. Goldblatt, J. Warren et al., “Pointing and stabilization system for use in a high altitude hovering helicopter,” in *Acquisition, Tracking, and Pointing XIII*, vol. 3692 of *Proceedings of SPIE*, pp. 23–32, Orlando, Fla, USA, April 1999.
[5] L.-M. Wang, W.-Q. Ge, and M.-J. Xie, “Neural network adaptive control method for speed ring of gyroscope stabilized platform,” *Opto-Electronic Engineering*, vol. 28, no. 4, pp. 9–12, 2001.
[6] J. Yan, J. Tang, and W. Shi, “FUZZY control on ship-borne radar stable platform servo system,” *Journal of China Ordnance*, vol. 20, no. 2, pp. 182–185, 1999.
[7] J. A. R. Krishna Moorty, R. Marathe, and V. R. Sule, “H_∞ control law for line-of-sight stabilization for mobile land vehicles,” *Optical Engineering*, vol. 41, no. 11, pp. 2935–2944, 2002.
[8] W. J. Bigley and S. P. Tsao, “Optimal motion stabilization control of an electro-optical sight system,” in *Acquisition, Tracking, and Pointing III*, vol. 1111 of *Proceedings of SPIE*, pp. 116–120, Orlando, Fla, USA, March 1989.
[9] L. Zhang, C. Wang, and L. Chen, “Stability and stabilization of a class of multimode linear discrete-time systems with polytopic uncertainties,” *IEEE Transactions on Industrial Electronics*, vol. 56, no. 9, pp. 3684–3692, 2009.
[10] L. Zhang and E. Boukas, “Stability and stabilization of Markovian jump linear systems with partly unknown transition probabilities,” *Automatica*, vol. 45, no. 2, pp. 463–468, 2009.
[11] L. Zhang, E. Boukas, and J. Lam, “Analysis and synthesis of Markov jump linear systems with time-varying delays and partially known transition probabilities,” *IEEE Transactions on Automatic Control*, vol. 53, no. 10, pp. 2458–2464, 2008.
[12] K. Zhou, *Essentials of Robust Control*, Prentice-Hall, Englewood Cliffs, NJ, USA, 1998.
[13] P. Gahinet and P. Apkarian, “A linear matrix inequality approach to H_∞ control,” *International Journal of Robust and Nonlinear Control*, vol. 4, no. 4, pp. 421–448, 1994.
[14] R. E. Skelton, T. Iwasaki, and K. Grigoriadis, *A Unified Approach to Linear Control Design*, Taylor & Francis, New York, NY, USA, 1997.
[15] T. T. Georgiou, “The interpolation problem with a degree constraint,” *IEEE Transactions on Automatic Control*, vol. 44, no. 3, pp. 631–635, 1999.
[16] C. J. Byrnes, T. T. Georgiou, and A. Lindquist, “A generalized entropy criterion for Nevanlinna-Pick interpolation with degree constraint,” *IEEE Transactions on Automatic Control*, vol. 46, no. 6, pp. 822–839, 2001.
[17] C. I. Byrnes, T. T. Georgiou, A. Lindquist, and A. Megretski, “Generalized interpolation in H^∞ with a complexity constraint,” *Transactions of the American Mathematical Society*, vol. 358, no. 3, pp. 965–987, 2006.
[18] C. I. Byrnes, T. T. Georgiou, and A. Lindquist, “Analytic interpolation with degree constraint: a constructive theory with applications to control and signal processing,” in *Proceedings of the 38th IEEE Conference on Decision and Control (CDC ’99)*, vol. 1, pp. 982–988, Phoenix, Ariz, USA, December 1999.
[19] R. Nagamune, “A robust solver using a continuation method for Nevanlinna-Pick interpolation with degree constraint,” *IEEE Transactions on Automatic Control*, vol. 48, no. 1, pp. 113–117, 2003.
[20] A. Tannenbaum, “Feedback stabilization of linear dynamical plants with uncertainty in the gain factor,” *International Journal of Control*, vol. 32, no. 1, pp. 1–16, 1980.
[21] P. P. Khargonekar and A. Tannenbaum, “Non-Euclidean metrics and the robust stabilization of systems with parameter uncertainty,” *IEEE Transactions on Automatic Control*, vol. 30, no. 10, pp. 1005–1013, 1985.
[22] D. J. N. Limebeer and B. D. O. Anderson, “An interpolation theory approach to H^∞ controller degree bounds,” *Linear Algebra and Its Applications*, vol. 98, pp. 347–386, 1988.
[23] J. W. Helton and O. Merino, *Classical Control Using H_∞ Methods. Theory, Optimization, and Design*, SIAM, Philadelphia, Pa, USA, 1998, .
[24] J. L. Walsh, *Interpolation and Approximation by Rational Functions in the Complex Domain*, American Mathematical Society Colloquium Publications, American Mathematical Society, Providence, RI, USA, 1956.
[25] R. Nagamune, “Closed-loop shaping based on Nevanlinna-Pick interpolation with a degree bound,” *IEEE Transactions on Automatic Control*, vol. 49, no. 2, pp. 300–305, 2004.


Advances in
Operations Research
Advances in
Decision Sciences
Journal of
Applied Mathematics
Algebra
Journal of
Probability and Statistics
The Scientific
World Journal
Hindawi
Submit your manuscripts at
http://www.hindawi.com
International Journal of
Differential Equations
International Journal of
Combinatorics
Advances in
Mathematical Physics
Journal of
Complex Analysis
Journal of
Mathematics
Mathematical Problems
in Engineering
Abstract and
Applied Analysis
Discrete Dynamics in
Nature and Society
International
Journal of
Mathematics and
Mathematical
Sciences
Journal of
Discrete Mathematics
Journal of
Function Spaces
International Journal of
Stochastic Analysis
Journal of
Optimization